Research Square

Preprints are preliminary reports that have not undergone peer review.
They should not be considered conclusive, used to inform clinical practice,
or referenced by the media as validated information.

PROM1 and RAC1/PAK1 Transcript Responses to Extracellular Vesicle Preparations from Cancer-Associated Fibroblasts in SW480 Cells

Parisa Sabzi
Islamic Azad University, Science and Research Branch
Masoumeh Hosseini
Tarbiat Modares University
Roudabeh Behzadi Andouhjerdi
Islamic Azad University, Science and Research Branch
Mahsa Damghanian
Islamic Azad University, Science and Research Branch
Zeinab Piravar
Z.Piravar@iau.ac.ir

Islamic Azad University, Science and Research Branch
Sadegh Babashah
Tarbiat Modares University

Research Article

Keywords: Colorectal cancer, cancer-associated fibroblasts, extracellular vesicles, PROM1 (CD133), RAC1, PAK1

Posted Date: November 13th, 2026

DOI: https://doi.org/10.21203/rs.3.rs-11509910/v1

License: This work is licensed under a Creative Commons Attribution 4.0 International License.
Read Full License

Additional Declarations: No competing interests reported.

PROM1 and RAC1/PAK1 Transcript Responses to Extracellular Vesicle Preparations from Cancer-Associated Fibroblasts in SW480 Cells

Parisa Sabzi[1], Masoumeh Hosseini[2], Roudabeh Behzadi Andouhjerdi[1], Mahsa Damghanian[1], Zeinab Piravar[1]*, Sadegh Babashah[3]*

[1] Department of Biology, Central Tehran Branch, Islamic Azad University, Tehran, Iran

[2] Department of Immunology, Faculty of Medical Sciences, Tarbiat Modares University, Tehran, Iran

[3] Department of Molecular Genetics, Faculty of Biological Sciences, Tarbiat Modares University, Tehran, Iran

Corresponding authors: Zeinab Piravar, Ph.D. (Saba.Piravar@gmail.com; Z.Piravar@iau.ac.ir); Sadegh Babashah, Ph.D. (sadegh.babashah@gmail.com; babashah@modares.ac.ir)

Running title: CAF-derived EV preparations and SW480 transcripts

Conflict of interest statement: The authors declare no potential conflicts of interest.

Abstract

Cancer-associated fibroblast (CAF)-derived extracellular vesicles (EVs) have been implicated in colorectal cancer progression, but their associations with PROM1 and RAC1/PAK1 expression remain incompletely characterized. We examined the effects of CAF-derived EV preparations on metabolic activity and selected stemness- and epithelial–mesenchymal transition (EMT)-related transcripts in SW480 colorectal cancer cells. Preparations were obtained by ExoQuick precipitation, assessed by dynamic light scattering (DLS), and applied at 100 µg/mL for 48 h. 3-(4,5-Dimethylthiazol-2-yl)-2,5-diphenyltetrazolium bromide (MTT) assays measured metabolic activity, and quantitative real-time PCR (qRT-PCR) measured relative PROM1, SNAI1, ZEB1, RAC1, and PAK1 mRNA levels. Separate experimental arms evaluated small interfering RNAs (siRNAs) targeting PROM1 or RAC1 (siPROM1 and siRAC1, respectively), each at 30 nM. Treatment with the preparations increased MTT activity and the expression of all five transcripts relative to untreated controls. siPROM1 and siRAC1 reduced their respective target mRNAs. In the PROM1 arm, ZEB1 and SNAI1 transcript levels and MTT activity were numerically lower in cells receiving EV preparations with siPROM1 than in cells receiving the preparations alone. In the RAC1 arm, PAK1 transcript levels and MTT activity were numerically lower with combined EV preparation and siRAC1 treatment than with preparations alone. These observations describe exploratory transcript-level and metabolic responses in a single colorectal cancer cell model and provide a basis for targeted functional validation.

Keywords: Colorectal cancer; cancer-associated fibroblasts; extracellular vesicles; PROM1 (CD133); RAC1; PAK1.

Introduction

Colorectal cancer (CRC) is the third most commonly diagnosed malignancy and the second leading cause of cancer-related death worldwide (1). Recurrence, metastasis, and treatment resistance remain major clinical challenges (2, 3). Alongside genetic alterations, interactions between tumor cells and the tumor microenvironment (TME) contribute to CRC progression (4-6).

Cancer-associated fibroblasts (CAFs) are a major stromal component of the TME. Through secreted factors, extracellular matrix components, and extracellular vesicles (EVs), they influence angiogenesis, invasion, metastasis, stemness, epithelial–mesenchymal transition (EMT), and drug resistance (7-10). EVs carry proteins, lipids, and regulatory RNAs that can alter signaling in recipient cells (11, 12).

Cancer stem cells (CSCs) contribute to tumor initiation, treatment resistance, and recurrence (13, 14). Prominin-1 (CD133) is a widely used CSC marker associated with stemness and tumorigenic potential (15-17), and small interfering RNAs (siRNAs) allow stemness-associated genes to be examined through targeted suppression (17-19). EMT contributes to tumor cell plasticity and invasion and is regulated by transcription factors that include Snail and ZEB1 (20, 21). These observations provide a rationale for examining PROM1 expression alongside SNAI1 and ZEB1 in CRC cells.

Rac1 and its downstream effector PAK1 also participate in CRC progression (22, 23). Their functions include the regulation of cytoskeletal remodeling, migration, proliferation, invasion, and EMT (24). Dysregulated Rac1 expression and activity have been associated with advanced disease, metastasis, and poor outcomes (25-28).

CAF-derived EVs have been implicated in stemness, EMT, and treatment responses in CRC (29, 30). Within this context, we examined changes in PROM1, SNAI1, ZEB1, RAC1, and PAK1 mRNA levels and MTT metabolic activity in SW480 cells exposed to CAF-derived EV preparations. Two separate siRNA experiments examined the PROM1-related and RAC1/PAK1-related transcript responses after siPROM1 or siRAC1 transfection, respectively.

Materials and Methods

Cell culture

SW480 human colorectal cancer cells (RRID:CVCL_0546) were obtained from the Pasteur Institute cell bank and cultured in DMEM/F12 supplemented with 10% fetal bovine serum (FBS) and 1% penicillin/streptomycin at 37°C in a humidified atmosphere containing 5% CO_2. The medium was replaced every 48–72 h, and cells were subcultured at approximately 80–90% confluence (31).

Cancer-associated fibroblast (CAF) culture

Human cancer-associated fibroblasts (CAFs) were provided by the Department of Genetics, Tarbiat Modares University. Cells were cultured in complete DMEM at 37°C under 5% CO_2. Cultures were monitored for mycoplasma using the MycoAlert Mycoplasma Detection Kit (Lonza, Walkersville, USA), and cell morphology was examined daily (32). Conditioned medium was collected at approximately 80% confluence for preparation of CAF-derived EV fractions with the ExoQuick kit (System Biosciences, USA) (33).

Preparation of CAF-derived extracellular vesicle fractions

CAF-derived extracellular vesicle (EV) fractions were prepared from conditioned medium using the ExoQuick precipitation kit (System Biosciences, USA). The medium was centrifuged to remove cells and cellular debris, mixed with the precipitation reagent, and centrifuged to recover the EV-enriched precipitate. The resulting pellet was resuspended in phosphate-buffered saline (PBS) and stored at −80°C (33-35).

Particle-size characterization

The preparations were diluted in PBS at a ratio of 1:6 and analyzed by dynamic light scattering (DLS) using a Zetasizer (Malvern, UK). Particle-size distributions were processed with Malvern Zetasizer software (version 7.11) (36). Throughout this manuscript, the term “EV preparation” refers to the ExoQuick-precipitated fraction from CAF-conditioned medium; DLS provides size information but does not establish vesicle identity or purity.

Treatment of SW480 cells

SW480 cells were incubated overnight to allow attachment and then treated with CAF-derived EV preparations at 100 µg/mL for 48 h. Untreated cells served as the negative control (37). This dose and exposure time fall within the range used for MSC-derived small EVs in colorectal cancer cells in a previous study from our laboratory (64).

Small interfering RNA (siRNA) transfection

SW480 cells were transfected separately with siPROM1 or siRAC1 using Lipofectamine™ 3000 (Thermo Fisher Scientific, USA) to assess transcript responses associated with suppression of the respective targets. Cells were grown to approximately 60–70% confluence. The siRNA–Lipofectamine mixture was prepared in serum-free medium and added to the cells (38). A working siRNA concentration of 30 nM was selected from the MTT concentration-response experiments. At this concentration, siRNA treatment alone yielded approximately 52% of the untreated-control MTT signal; dose selection was based on metabolic activity rather than a concentration-dependent assessment of gene knockdown.

Experimental treatment groups

The PROM1 and RAC1 experiments were conducted separately. The PROM1 experiment included four groups: control (untreated), EV, siPROM1, and EV + siPROM1. The RAC1 experiment included control (untreated), EV, siRAC1, and EV + siRAC1 groups. siPROM1 and siRAC1 were not combined in any experimental group. In the combined-treatment groups, EV preparations and siRNA were added simultaneously. The EV group labels refer to the CAF-derived EV preparation.

MTT metabolic activity assay

The 3-(4,5-dimethyl-2-thiazolyl)-2,5-diphenyl-2-H-tetrazolium bromide (MTT) assay was used to assess cellular metabolic activity as an indicator of viability. For siRNA concentration screening, cells were seeded into 96-well plates in complete RPMI-1640 medium and incubated for one day. Cells were then transfected with siPROM1 or siRAC1 at 0, 10, 20, 30, or 40 nM using Lipofectamine™ 3000 (Thermo Fisher Scientific, USA). After two days, cells were incubated with MTT solution (5 mg/mL; Sigma-Aldrich, USA) for 4 h. Formazan crystals were dissolved in DMSO (Sigma-Aldrich, USA), and absorbance was measured at 570 nm using a spectrophotometer (Anthos, Austria). The MTT assays were performed in triplicate. In the separate four-condition experiments, MTT activity was compared among the untreated control, EV, siRNA, and EV + siRNA groups. Concentration-screen values and four-group fold-change values represent different comparisons and should not be interpreted as identical measurements. Data were analyzed using GraphPad Prism (39).

RNA extraction and quantitative real-time PCR (qRT-PCR)

After 48 h of treatment or transfection, total RNA was extracted from SW480 cells using TRIzol reagent according to the manufacturer's instructions. RNA concentration and purity were measured with a NanoDrop spectrophotometer (Thermo Fisher Scientific, USA). One microgram of total RNA was reverse-transcribed using a first-strand cDNA synthesis kit (Takara Biotechnology, Japan). PROM1 (CD133), ZEB1, SNAI1, RAC1, and PAK1 mRNA levels were quantified using SYBR Green Master Mix (Ampliqon, Denmark) on a StepOnePlus Real-Time PCR System (Applied Biosystems, USA). GAPDH was used as the endogenous reference gene, and relative expression was calculated by the $2^{-\Delta\Delta Ct}$ method. Three independent biological replicates were analyzed, with each sample measured in technical duplicate (40). Melting-curve analyses documented for PROM1, ZEB1, and SNAI1 were used to evaluate amplification specificity for those assays. Primer sequences are provided in Table 1.

Table 1. Primer sequences used for quantitative real-time PCR (qRT-PCR).

Gene	Forward primer (5′→3′)	Reverse primer (5′→3′)
PROM1 (CD133)	CACTACCCAAGGACAAGGCGTTC	CAACGCCTCTTTGGTCTCCTTG
ZEB1	GGCATACACCTACTCAACTACGG	TGGGCGGTGTAGAATCAGAGTC
SNAI1 (Snail)	TGCCCTCAAGATGCACATCCGA	GGGACAGGAGAAGGGCTTCTC
RAC1	CCCTATCCTATCCGCAAACA	CGCACCTCAGGATACCACTT
PAK1	AAGACATCCAACAGCCAGAA	TGTAGCCACGTCCCGAGT
GAPDH	ACACCCACTCCTCCACCTTTG	TCCACCACCCTGTTGCTGTAG

The RAC1 and PAK1 primer sequences were taken from Zhou et al. (41).

Statistical analysis

Experiments were performed in triplicate, and data are presented as mean ± standard deviation (SD). For qRT-PCR, three independent biological replicates were analyzed, with each sample measured in technical duplicate. MTT assays were performed in triplicate. Statistical analyses were performed in GraphPad Prism 9.4 (GraphPad Software Inc., San Diego, CA, USA). Group comparisons were analyzed using one-way analysis of variance (ANOVA) followed by Tukey's multiple-comparisons test, as applicable. For comparisons involving two groups, a one-factor ANOVA is equivalent to the conventional pooled-variance two-sample t-test. $P < 0.05$ was considered statistically significant. Asterisks in the figures indicate the annotated comparisons. The EV-only versus EV + siRNA contrasts are described descriptively, without a claim of statistical significance, because no corresponding pairwise result is available.

Results

Cell morphology and particle size of CAF-derived EV preparations

Phase-contrast microscopy showed spindle-shaped, fibroblast-like CAFs (Fig. 1A) and epithelial-like SW480 cells (Fig. 1B). DLS analysis of the CAF-derived EV preparations showed a particle-size peak at approximately 110 nm (Fig. 1C). Figure 1D summarizes the preparation of the conditioned-medium fraction, treatment of SW480 cells, and downstream analyses.

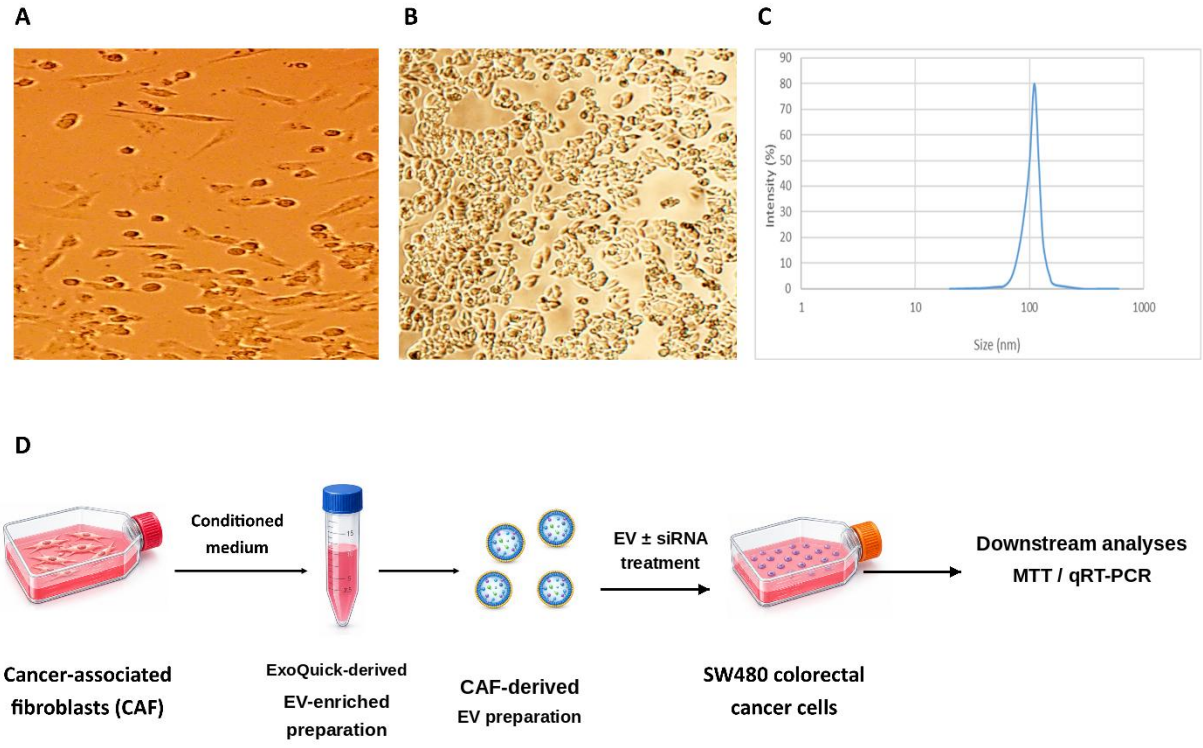


Figure 1. Cell morphology, particle-size distribution, and experimental workflow. (A) Spindle-shaped, fibroblast-like morphology of CAFs. (B) Epithelial-like morphology of SW480 cells. (C) DLS size distribution of the CAF-derived EV-enriched preparation, with a peak at approximately 110 nm. (D) Schematic of preparation of the conditioned-medium fraction, simultaneous exposure to the EV preparation and target-specific siRNA in the combined-treatment groups, and subsequent MTT and qRT-PCR analyses. The schematic indicates experimental stages and is not evidence of direct EV uptake or vesicle purity.

Selection of the siRNA concentration

In the siRNA concentration screens, MTT metabolic activity declined with increasing concentrations of siPROM1 or siRAC1 (Fig. 2A, B). At 30 nM, 52.44% of the untreated-control MTT signal remained for siPROM1 and 52.02% for siRAC1; the 30 nM concentration was used in subsequent experiments. These screening results are distinct from the fold-change values in the four-condition experiments and do not quantify gene-silencing efficiency.

PROM1-related transcript responses and metabolic activity

qRT-PCR showed significantly higher PROM1 mRNA levels in SW480 cells treated with CAF-derived EV preparations than in untreated controls (**$P < 0.01$; Fig. 2C). In the separate transfection comparison, PROM1 mRNA levels were significantly lower in siPROM1-transfected cells than in untreated cells (**$P < 0.01$; Fig. 2D).

MTT activity was compared among the control, EV, siPROM1, and EV + siPROM1 groups. Activity was higher in the EV group and lower in the siPROM1 group than in the untreated

control (*P < 0.05 versus control for both; Fig. 2E). The EV + siPROM1 group showed numerically lower MTT activity than the EV group. This assay reports metabolic activity and was not used as a direct measure of cell proliferation.

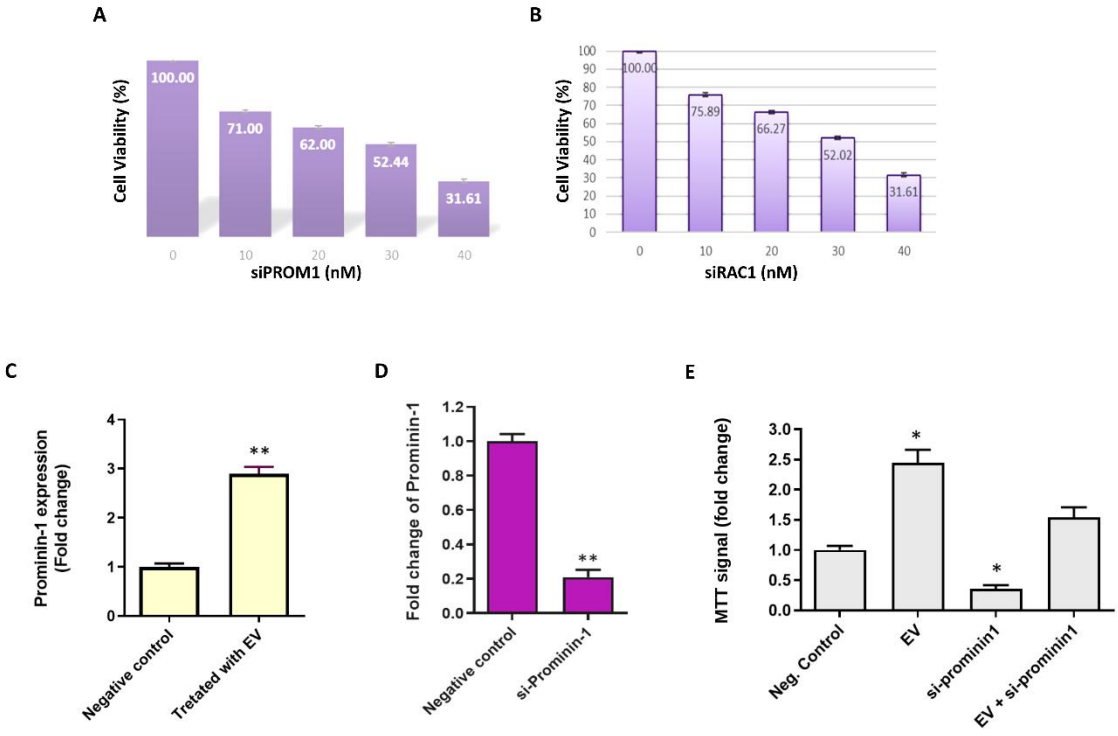


Figure 2. MTT metabolic activity and PROM1 transcript responses in SW480 cells. (A, B) MTT concentration-response profiles for siPROM1 (A) and siRAC1 (B). (C) PROM1 mRNA levels after treatment with the CAF-derived EV preparation. (D) PROM1 mRNA levels after siPROM1 transfection. (E) MTT signal (fold change) for untreated control, EV, siPROM1 and EV + siPROM1 groups. Concentration-screen and four-group MTT results are separately normalized datasets and are not directly interchangeable. For qRT-PCR, three independent biological replicates were measured in technical duplicate; MTT experiments were performed in triplicate. Results are presented as mean ± SD. Asterisks indicate the comparisons annotated in the panels (*P < 0.05; **P < 0.01); no EV-versus-combined-treatment P value is assigned.

ZEB1 and SNAI1 mRNA levels were also measured in the control, EV, siPROM1, and EV + siPROM1 groups. Both transcripts were higher in the EV group and lower in the siPROM1 group than in untreated controls (*P < 0.05 versus control; Fig. 3). The EV + siPROM1 group showed numerically lower ZEB1 and SNAI1 mRNA levels than the EV group.

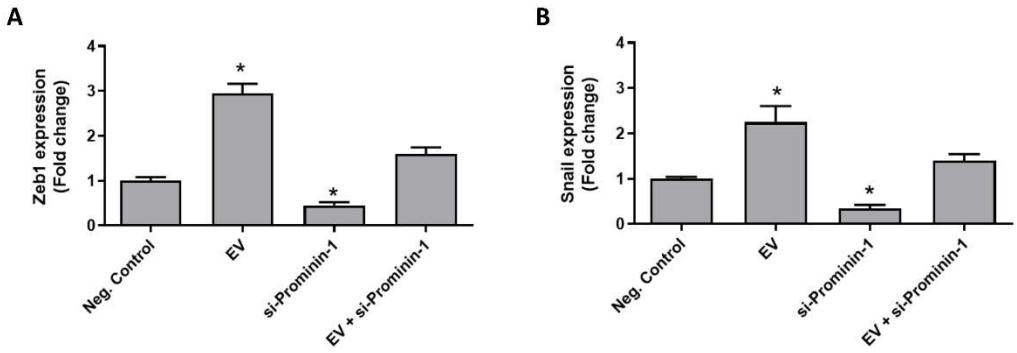


Figure 3. PROM1-associated EMT transcript responses in SW480 cells. Relative mRNA levels of (A) ZEB1 and (B) SNAI1 (Snail) after EV preparation exposure, siPROM1 transfection or combined treatment. Expression was measured by qRT-PCR and normalized to GAPDH. Three independent biological replicates were analyzed in technical duplicate; data are mean ± SD. *P < 0.05 indicates the comparisons annotated in the plots; differences between EV-only and combined treatment are descriptive.

RAC1 and PAK1 transcript responses and metabolic activity

RAC1 mRNA levels, measured by qRT-PCR, were significantly higher in SW480 cells treated with CAF-derived EV preparations than in untreated cells (**P < 0.01; Fig. 4A). In the separate transfection comparison, RAC1 mRNA levels were significantly lower in siRAC1-transfected cells than in untreated cells (**P < 0.01; Fig. 4B).

MTT activity was compared among the control, EV, siRAC1, and EV + siRAC1 groups. Activity was higher in the EV group and lower in the siRAC1 group than in untreated controls (*P < 0.05 versus control for both; Fig. 4C). The EV + siRAC1 group showed numerically lower MTT activity than the EV group.

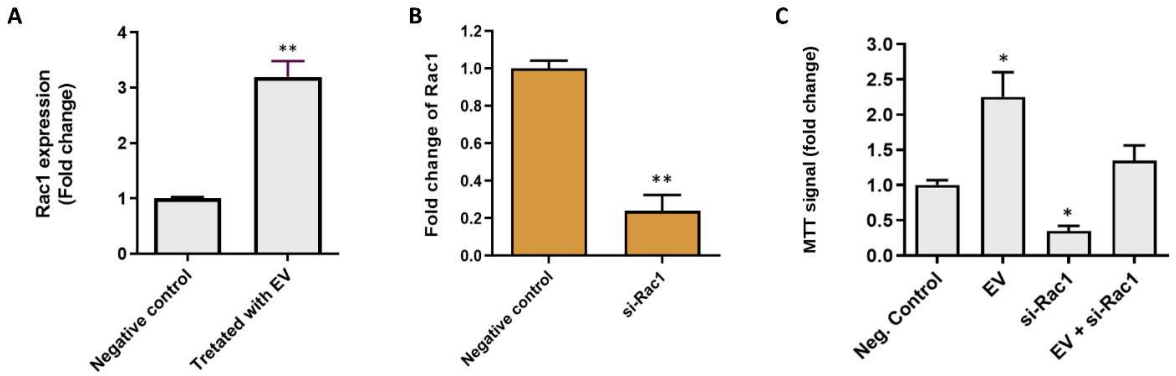


Figure 4. RAC1 transcript responses and MTT metabolic activity in SW480 cells. (A) RAC1 mRNA expression after exposure to the CAF-derived EV preparation. (B) RAC1 mRNA expression after siRAC1 transfection. (C) MTT signal (fold change) in untreated control, EV, siRAC1 and EV + siRAC1 groups. For qRT-PCR, three independent biological replicates were analyzed in technical duplicate; MTT experiments were performed in triplicate. Data are mean ± SD. Asterisks indicate the comparisons annotated in the plots (*P < 0.05; **P < 0.01); no EV-versus-combined-treatment P value is assigned.

PAK1 mRNA levels were measured by qRT-PCR in the control, EV, siRAC1, and EV + siRAC1 groups. Levels were higher in the EV group and lower in the siRAC1 group than in untreated controls (*P < 0.05 versus control for both; Fig. 5). The EV + siRAC1 group showed numerically lower PAK1 mRNA levels than the EV group.

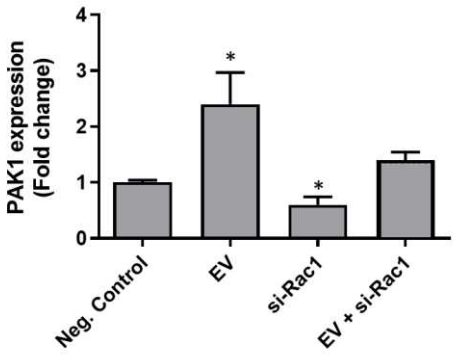


Figure 5. PAK1 transcript responses in SW480 cells. Relative PAK1 mRNA expression in the untreated control, EV, siRAC1 and EV + siRAC1 groups. Expression was measured using qRT-PCR and normalized to GAPDH. Three independent biological replicates were analyzed in technical duplicate; data are mean ± SD. *P < 0.05 indicates the comparisons annotated in the plot; differences between EV-only and combined treatment are descriptive.

Discussion

Recurrence, metastasis, and treatment resistance continue to limit outcomes in CRC (42, 43). Interactions between tumor cells and the stromal and immune components of the TME contribute to these challenges (44, 45). Studies in other epithelial cancers have linked CAF-derived EVs to migration and invasion (46). EV-mediated communication can occur in both directions between fibroblasts and tumor cells (47), while cancer-cell-derived EVs may also contribute to the diversity of CAF subtypes (48).

In SW480 cells, exposure to CAF-derived EV preparations was associated with increased PROM1, RAC1, PAK1, ZEB1, and SNAI1 mRNA levels and increased MTT metabolic activity compared with untreated controls. In the siPROM1 arm, ZEB1 and SNAI1 mRNA levels were numerically lower during combined treatment than with EV preparations alone; in the siRAC1 arm, the corresponding pattern involved PAK1. MTT activity was also numerically lower in both combined-treatment groups. These findings indicate preparation-associated transcript and metabolic responses, without demonstrating a shared signaling pathway or a causal requirement for either target.

Prominin-1 (CD133) is recognized as a marker and functional regulator of colorectal cancer stem cells (49). It has been linked to stem cell maintenance, self-renewal, treatment resistance, and cellular states that favor EMT (50, 51). ZEB1 and Snail regulate epithelial and mesenchymal gene expression and contribute to cellular plasticity and invasion (52). Here, siPROM1 reduced

PROM1 mRNA, and the EV + siPROM1 group showed numerically lower ZEB1 and SNAI1 transcript levels and MTT metabolic activity than the EV group. These findings associate the siPROM1 treatment condition with EMT-related transcript responses; they do not demonstrate PROM1-specific regulation of functional EMT.

Rac1 signals through PAK1, a serine/threonine kinase involved in actin dynamics, focal adhesion turnover, migration, and proliferation (53-55). Rac1/PAK1 signaling has also been linked to EMT-related transcription factors and pathways, including MAPK/ERK, NF-κB, and β-catenin (26, 56-59). In other tumor models, RAC1 silencing has reduced migration and invasion (60, 61). In the present RAC1 arm, siRAC1 reduced RAC1 mRNA, while PAK1 mRNA and MTT metabolic activity were numerically lower with EV + siRAC1 than with the EV preparation alone. These transcript and metabolic observations do not establish RAC1-GTP loading, PAK1 phosphorylation, or pathway activation.

Evidence from other tumor models links Rac1/PAK1 activity to EMT programs, including Snail regulation (62, 63). This provides a biological context for considering a relationship between the two response patterns observed here. However, the experiments did not test the effects of siPROM1 on RAC1/PAK1 or of siRAC1 on ZEB1/SNAI1, so they provide no direct evidence of crosstalk.

Limitations

This exploratory study examined a single colorectal cancer cell line and principally measured transcript abundance and MTT metabolic activity. CAF-conditioned-medium fractions were prepared by ExoQuick precipitation and assessed by DLS without complementary vesicle-marker or ultrastructural characterization. Accordingly, EV-associated responses cannot be conclusively separated from effects of co-precipitated non-vesicular material. Uptake of the preparations by SW480 cells was not examined here, although uptake of labeled MSC-derived small EVs by colorectal cancer cells has been reported previously (64). Matched non-targeting siRNA and transfection-reagent-only controls were not included. In the siPROM1 dose-response screen, 30 nM siPROM1 reduced normalized MTT signal by approximately 48% relative to the untreated control; the separately presented four-group experiments also showed lower siRNA-only MTT signals, but their fold changes are not directly interchangeable with the screening percentages. Silencing efficiency was shown for siPROM1 and siRAC1 versus untreated control, but target knockdown was not independently demonstrated within the combined EV + siRNA treatment groups. The method used to assign a protein-equivalent concentration to the EV preparations and the use of EV-depleted serum during CAF-conditioned-medium collection were not specified in the source protocol. Protein abundance, RAC1-GTP loading, PAK1 phosphorylation, functional EMT, and experimental crosstalk between the separate PROM1 and RAC1 arms were not directly assessed.

Conclusion

CAF-derived EV-enriched preparations were associated with increased PROM1, RAC1, PAK1, ZEB1, and SNAI1 mRNA levels and higher MTT metabolic activity in SW480 cells. In the separate siPROM1 and siRAC1 experiments, the corresponding combined-treatment groups showed numerically lower EMT-related or PAK1 transcript levels and MTT responses than the EV-only groups. These findings provide a descriptive basis for further experiments but do not establish EV-specific causality, functional pathway activation, or direct crosstalk between the two gene-response modules.

Declarations

Ethics approval and consent to participate

The study was approved by the Ethics Committee of Islamic Azad University (approval No. IR.IAU.CTB.REC.1404.082). SW480 cells were obtained from the Pasteur Institute cell bank, while cancer-associated fibroblast cultures were provided by the Department of Genetics, Tarbiat Modares University. The experiments used cultured cells; no participants were recruited directly and no identifiable participant information was analyzed.

Author Contributions

P.S. performed SW480 cell culture, siPROM1 transfection, MTT assays, and qRT-PCR analyses of PROM1, ZEB1, and SNAI1. M.H. contributed to the RAC1/PAK1-related experimental data and analyses. P.S. and M.H. prepared the original draft. M.D. contributed software-based analyses and formula calculations. Z.P. reviewed and edited the manuscript and supervised the study. S.B. contributed to study design, methodology, and supervision. R.B.A. supervised the project.

Funding

This research did not receive any specific grant from funding agencies in the public, commercial, or not-for-profit sectors.

Data Availability

The datasets generated and/or analyzed during the current study are available from the corresponding authors upon reasonable request.

Consent for Publication

Not applicable.

Competing Interests

The authors declare no potential conflicts of interest.

Clinical Trial Number

Not applicable.

References

1. Xi Y, Xu P. Global colorectal cancer burden in 2020 and projections to 2040. Translational oncology. 2021;14(10):101174.
2. Adebayo AS, Agbaje K, Adesina SK, Olajubutu O. Colorectal cancer: disease process, current treatment options, and future perspectives. Pharmaceutics. 2023;15(11):2620.
3. Qi G-X, Zhao R-X, Gao C, Ma Z-Y, Wang S, Xu J. Recent advances and challenges in colorectal cancer: From molecular research to treatment. World Journal of Gastroenterology. 2025;31(21):106964.
4. Giraldo NA, Sanchez-Salas R, Peske JD, Vano Y, Becht E, Petitprez F, et al. The clinical role of the TME in solid cancer. British journal of cancer. 2019;120(1):45-53.
5. Li J, Chen D, Shen M. Tumor microenvironment shapes colorectal cancer progression, metastasis, and treatment responses. Frontiers in medicine. 2022;9:869010.
6. Wu X, Yan H, Qiu M, Qu X, Wang J, Xu S, et al. Comprehensive characterization of tumor microenvironment in colorectal cancer via molecular analysis. Elife. 2023;12:e86032.
7. Li Z, Zhang J, Zhou J, Lu L, Wang H, Zhang G, et al. Nodal facilitates differentiation of fibroblasts to cancer-associated fibroblasts that support tumor growth in melanoma and colorectal cancer. Cells. 2019;8(6):538.
8. De Boeck A, Hendrix A, Maynard D, Van Bockstal M, Daniels A, Pauwels P, et al. Differential secretome analysis of cancer-associated fibroblasts and bone marrow-derived precursors to identify microenvironmental regulators of colon cancer progression. Proteomics. 2013;13(2):379-88.
9. Fotsitzoudis C, Koulouridi A, Messaritakis I, Konstantinidis T, Gouvas N, Tsiaoussis J, Souglakos J. Cancer-associated fibroblasts: The origin, biological characteristics and role in cancer—A glance on colorectal cancer. Cancers. 2022;14(18):4394.

10. Hu J, Wang W, Lan X, Zeng Z, Liang Y, Yan Y, et al. CAFs secreted exosomes promote metastasis and chemotherapy resistance by enhancing cell stemness and epithelial-mesenchymal transition in colorectal cancer. Molecular cancer. 2019;18(1):91.
11. Abels ER, Breakefield XO. Introduction to extracellular vesicles: biogenesis, RNA cargo selection, content, release, and uptake. Cellular and molecular neurobiology. 2016;36(3):301-12.
12. Shoucair I, Weber Mello F, Jabalee J, Maleki S, Garnis C. The role of cancer-associated fibroblasts and extracellular vesicles in tumorigenesis. International Journal of Molecular Sciences. 2020;21(18):6837.
13. Das PK, Islam F, Lam AK. The roles of cancer stem cells and therapy resistance in colorectal carcinoma. Cells. 2020;9(6):1392.
14. Gupta R, Bhatt LK, Johnston TP, Prabhavalkar KS. Colon cancer stem cells: Potential target for the treatment of colorectal cancer. Cancer biology & therapy. 2019;20(8):1068-82.
15. Huang JL, Oshi M, Endo I, Takabe K. Clinical relevance of stem cell surface markers CD133, CD24, and CD44 in colorectal cancer. American Journal of Cancer Research. 2021;11(10):5141.
16. Tirino V, Desiderio V, Paino F, De Rosa A, Papaccio F, Fazioli F, et al. Human primary bone sarcomas contain CD133+ cancer stem cells displaying high tumorigenicity in vivo. The FASEB Journal. 2011;25(6):2022-30.
17. Moreno-Londoño AP, Robles-Flores M. Functional roles of CD133: more than stemness associated factor regulated by the microenvironment. Stem cell reviews and reports. 2024;20(1):25-51.
18. Alemohammad H, Motafakkerazad R, Asadzadeh Z, Farsad N, Hemmat N, Najafzadeh B, et al. siRNA-mediated silencing of Nanog reduces stemness properties and increases the sensitivity of HepG2 cells to cisplatin. Gene. 2022;821:146333.
19. Lan X, Wu Y-Z, Wang Y, Wu F-R, Zang C-B, Tang C, et al. CD133 silencing inhibits stemness properties and enhances chemoradiosensitivity in CD133-positive liver cancer stem cells. International journal of molecular medicine. 2013;31(2):315-24.

20. Saitoh M, editor Transcriptional regulation of EMT transcription factors in cancer. Seminars in cancer biology; 2023: Elsevier.
21. Wang Y, Wu Z, Hu L. The regulatory effects of metformin on the [SNAIL/miR-34]:[ZEB/miR-200] system in the epithelial-mesenchymal transition (EMT) for colorectal cancer (CRC). European journal of pharmacology. 2018;834:45-53.
22. Zhu G, Wang Y, Huang B, Liang J, Ding Y, Xu A, Wu W. A Rac1/PAK1 cascade controls β-catenin activation in colon cancer cells. Oncogene. 2012;31(8):1001-12.
23. Kotelevets L, Chastre E. Rac1 signaling: from intestinal homeostasis to colorectal cancer metastasis. Cancers. 2020;12(3):665.
24. De P, Aske JC, Dey N. RAC1 takes the lead in solid tumors. Cells. 2019;8(5):382.
25. Zhou K, Rao J, Zhou Z-h, Yao X-h, Wu F, Yang J, et al. RAC1-GTP promotes epithelial-mesenchymal transition and invasion of colorectal cancer by activation of STAT3. Laboratory investigation. 2018;98(8):989-98.
26. Xia L, Lin J, Su J, Oyang L, Wang H, Tan S, et al. Diallyl disulfide inhibits colon cancer metastasis by suppressing Rac1-mediated epithelial-mesenchymal transition. OncoTargets and therapy. 2019:5713-28.
27. Gao X, Xu W, Lu T, Zhou J, Ge X, Hua D. MicroRNA-142-3p promotes cellular invasion of colorectal cancer cells by activation of RAC1. Technology in cancer research & treatment. 2018;17:1533033818790508.
28. Lou S, Wang P, Yang J, Ma J, Liu C, Zhou M. Prognostic and clinicopathological value of Rac1 in cancer survival: evidence from a meta-analysis. Journal of Cancer. 2018;9(14):2571.
29. Lin Z, Li G, Jiang K, Li Z, Liu T. Cancer therapy resistance mediated by cancer-associated fibroblast-derived extracellular vesicles: biological mechanisms to clinical significance and implications. Molecular Cancer. 2024;23(1):191.

30. Hjazi A, Saleh RO, Al-Khafaji ZA, Alkhathami AG, Kundlas M, Maharana L, et al. Exosomal Dialogue: The Emerging Role of Cancer-Associated Fibroblast-Derived Exosomes in Colorectal Cancer Progression and Therapy Resistance. Journal of Biochemical and Molecular Toxicology. 2026;40(4):e70780.
31. Murthy KNC, Jayaprakasha GK, Patil BS. The natural alkaloid berberine targets multiple pathways to induce cell death in cultured human colon cancer cells. European journal of pharmacology. 2012;688(1-3):14-21.
32. Magan M, Wiechec E, Roberg K. CAFs affect the proliferation and treatment response of head and neck cancer spheroids during co-culturing in a unique in vitro model. Cancer Cell International. 2020;20(1):599.
33. Lee S-S, Won J-H, Lim GJ, Han J, Lee JY, Cho K-O, Bae Y-K. A novel population of extracellular vesicles smaller than exosomes promotes cell proliferation. Cell Communication and Signaling. 2019;17(1):95.
34. Wu S-C, Kuo P-J, Rau C-S, Wu Y-C, Wu C-J, Lu T-H, et al. Subpopulations of exosomes purified via different exosomal markers carry different microRNA contents. International Journal of Medical Sciences. 2021;18(4):1058.
35. Yang Y, Wang Y, Wei S, Zhou C, Yu J, Wang G, et al. Extracellular vesicles isolated by size-exclusion chromatography present suitability for RNomics analysis in plasma. Journal of translational medicine. 2021;19(1):104.
36. Hosseini M, Ezzeddini R, Hashemi SM, Soudi S, Salek Farrokhi A. Enhanced anti-tumor efficacy of S3I-201 in breast cancer mouse model through Wharton jelly-exosome. Cancer Cell International. 2024;24(1):318.
37. Ding Y, Zhao H, Niu W, Zhang J, Zheng X, Liu Y, et al. M2 macrophage-derived extracellular vesicles containing MicroRNA-501-3p promote colon cancer progression through the SETD7/DNMT1/SOCS3 axis. Diseases of the Colon & Rectum. 2023;66(12):e1234-e45.

38. Niu X, Pu S, Ling C, Xu J, Wang J, Sun S, et al. lncRNA Oip5-as1 attenuates myocardial ischaemia/reperfusion injury by sponging miR-29a to activate the SIRT1/AMPK/PGC1α pathway. Cell Proliferation. 2020;53(6):e12818.

39. Karami H, Baradaran B, Esfahani A, Estiar MA, Naghavi-Behzad M, Sakhinia M, Sakhinia E. siRNA-mediated silencing of survivin inhibits proliferation and enhances etoposide chemosensitivity in acute myeloid leukemia cells. Asian Pacific Journal of Cancer Prevention. 2013;14(12):7719-24.

40. Davudian S, Shajari N, Kazemi T, Mansoori B, Salehi S, Mohammadi A, et al. BACH1 silencing by siRNA inhibits migration of HT-29 colon cancer cells through reduction of metastasis-related genes. Biomedicine & pharmacotherapy. 2016;84:191-8.

41. Zhou Y, Su J, Shi L, Liao Q, Su Q. DADS downregulates the Rac1-ROCK1/PAK1-LIMK1-ADF/cofilin signaling pathway, inhibiting cell migration and invasion. Oncology Reports. 2013;29(2):605-12.

42. Siegel RL, Wagle NS, Cercek A, Smith RA, Jemal A. Colorectal cancer statistics, 2023. CA: a cancer journal for clinicians. 2023;73(3):233-54.

43. Kumar A, Gautam V, Sandhu A, Rawat K, Sharma A, Saha L. Current and emerging therapeutic approaches for colorectal cancer: A comprehensive review. World Journal of Gastrointestinal Surgery. 2023;15(4):495.

44. De Visser KE, Joyce JA. The evolving tumor microenvironment: From cancer initiation to metastatic outgrowth. Cancer cell. 2023;41(3):374-403.

45. Wang Q, Shao X, Zhang Y, Zhu M, Wang FX, Mu J, et al. Role of tumor microenvironment in cancer progression and therapeutic strategy. Cancer medicine. 2023;12(10):11149-65.

46. Dourado MR, Korvala J, Åström P, De Oliveira CE, Cervigne NK, Mofatto LS, et al. Extracellular vesicles derived from cancer-associated fibroblasts induce the migration and invasion of oral squamous cell carcinoma. Journal of extracellular vesicles. 2019;8(1):1578525.

47. Santi A, Moccia A, Caselli A, Cirri P. EV-mediated asymmetrical crosstalk between CAFs and cancer cells in the tumor microenvironment. Biochimica et Biophysica Acta (BBA)-Reviews on Cancer. 2025;1880(4):189380.

48. Naito Y. How Do Cancer Cells Create Cancer-Associated Fibroblast Subtypes? Impacts of Extracellular Vesicles on Stromal Diversity. Cancer Science. 2025;116(9):2347-61.

49. Ren F, Sheng W-Q, Du X. CD133: a cancer stem cells marker, is used in colorectal cancers. World journal of gastroenterology: WJG. 2013;19(17):2603.

50. Yuan Z, Liang X, Zhan Y, Wang Z, Xu J, Qiu Y, et al. Targeting CD133 reverses drug-resistance via the AKT/NF-κB/MDR1 pathway in colorectal cancer. British journal of cancer. 2020;122(9):1342.

51. Park J, Kim SK, Hallis SP, Choi B-H, Kwak M-K. Role of CD133/NRF2 axis in the development of colon cancer stem cell-like properties. Frontiers in Oncology. 2022;11:808300.

52. Bastos VAF, Souza AGd, Guedes VCS, Cunha TM. Shared and context-specific mechanisms of EMT and cellular plasticity in cancer and fibrotic diseases. International journal of molecular sciences. 2025;26(19):9476.

53. Zhao H, Dong T, Zhou H, Wang L, Huang A, Feng B, et al. miR-320a suppresses colorectal cancer progression by targeting Rac1. Carcinogenesis. 2014;35(4):886-95.

54. Wufuer R, Ma H-X, Luo M-Y, Xu K-Y, Kang L. Downregulation of Rac1/PAK1/LIMK1/cofilin signaling pathway in colon cancer SW620 cells treated with Chlorin e6 photodynamic therapy. Photodiagnosis and photodynamic therapy. 2021;33:102143.

55. Ma N, Xu E, Luo Q, Song G. Rac1: a regulator of cell migration and a potential target for cancer therapy. Molecules. 2023;28(7):2976.

56. Yang L, Yang J, Liu H, Lan J, Xu Y, Wu X, et al. Minocycline binds and inhibits LYN activity to prevent STAT3-meditated metastasis of colorectal cancer. International journal of biological sciences. 2022;18(6):2540.

57. De P, Rozeboom BJ, Aske JC, Dey N. Active RAC1 promotes tumorigenic phenotypes and therapy resistance in solid tumors. Cancers. 2020;12(6):1541.

58. Ye DZ, Field J. PAK signaling in cancer. Cellular logistics. 2012;2(2):105-16.

59. Orgaz JL, Herraiz C, Sanz-Moreno V. Rho GTPases modulate malignant transformation of tumor cells. Small GTPases. 2014;5(4):e983867.

60. He Z, Song K, Han H, Wang L, Chen Z, Shang W. RAC1 promotes the occurrence and development of tongue squamous cell carcinoma by regulating RAC1/PAK1/LIMK1 signaling pathway. Scientific Reports. 2025;15(1):8831.

61. Chen Q-Y, Xu L-Q, Jiao D-M, Yao Q-H, Wang Y-Y, Hu H-Z, et al. Silencing of Rac1 modifies lung cancer cell migration, invasion and actin cytoskeleton rearrangements and enhances chemosensitivity to antitumor drugs. International journal of molecular medicine. 2011;28(5):769-76.

62. Li J, Zhu Y, Duan R, Tian Y, Li X, Song Y. Rac1 in gastric cancer: a molecular driver of invasion, EMT, and therapeutic resistance. Journal of Translational Medicine. 2025;23(1):1221.

63. Cao F, Yin L-X. PAK1 promotes proliferation, migration and invasion of hepatocellular carcinoma by facilitating EMT via directly up-regulating Snail. Genomics. 2020;112(1):694-702.

64. Behzadi Andouhjerdi R, Hosseini F, Hosseinzadeh N, Zivari S, Salkhordeh S, Mohammadi M, et al. Engineered mesenchymal stem cell-derived small extracellular vesicles delivering miR-124 suppress colorectal cancer progression through EZH2 downregulation and attenuation of STAT3 signaling. Medical Oncology. 2026;43:318. https://doi.org/10.1007/s12032-026-03418-z